American Mineralogist, Volume 79, pages 712–718, 1994

Characterization of the composition of fluid inclusions in minerals by ^1H NMR

Jean-Marie Dereppe
Unité CPMC, Université Catholique de Louvain la Neuve, Place Louis Pasteur 1, 1348 Louvain la Neuve, Belgium
Jacques Pironon
GDR CNRS-CREGU, BP 23, 54501 Vandœuvre-lès-Nancy, France
Claudette Moreaux
Unité CPMC, Université Catholique de Louvain la Neuve, Place Louis Pasteur 1, 1348 Louvain la Neuve, Belgium

Abstract

Synthetic (sylvite) and natural (quartz) crystals rich in aqueous and oil fluid inclusions have been studied by ^1H NMR spectroscopy. Separate crystals of each sample were analyzed using the MAS (magic angle spinning) NMR technique with a 90-MHz Bruker CXP spectrometer. The ^1H NMR spectra from synthetic inclusions of toluene and isobutylbenzene show H_2O and hydrocarbon contributions in separated spectral regions. The integrated intensities of each proton peak of the hydrocarbon fraction are in agreement with theoretical values. The sylvite crystals synthesized with an aliphatic natural oil have a ^1H MAS NMR spectrum showing the presence of H_2O, methyl, and methylene groups. For the same line broadening, the spectra recorded on free oil and on inclusions are similar. Ratios of $^1H_{ali}/^1H_{aro}$, CH_2/CH_3, and $CH/\Sigma C_{ali}$ can be calculated. Differences between the ratios measured on free oil and inclusions are due to poor resolution and to peak overlapping. The hydrocarbon-H_2O volumetric ratio varies from 3 to 10 vol% and is close to the measured value of 4 vol% of hydrocarbon. NMR has also been applied to natural inclusions in quartz crystals from the North Sea basin. Methane and aliphatic peaks have been detected, but no aromatic contribution has been observed. A methane concentration of 3.6 and 1.7 mol/L is estimated considering a pseudoaliphatic composition of *n*-nonane deduced from infrared data.

Introduction

Oil, gas, and water-bearing fluids may be trapped in intracrystalline microcavities (i.e., fluid inclusions) created during crystal growth or the healing of fractures. Various minerals can trap fluids; silicates (quartz, feldspar), sulfates (anhydrite), carbonates (calcite, dolomite), and halides (halite, fluorite) are commonly studied using optical methods. Oil-bearing minerals generally occur in sedimentary environments (e.g., sandstone, limestone, salt domes), although occurrences in metamorphic, hydrothermal, and igneous environments are known. Minerals from these last environments are rich in water and gas-bearing inclusions (CO_2, N_2, CH_4). Oil inclusions are ubiquitous in petroleum reservoirs and may be one phase (liquid or vapor), two phases (vapor bubble in a liquid phase), or three phases (vapor, liquid, and solid phases). Their composition and phase equilibrium are related to the *PVTX* conditions at the time of trapping. Comparisons can be made between the oil in the reservoir and the oil in the inclusions to determine the biodegradation or thermal degradation (or both) of the oil between the time of trapping and the present.

The chemical composition of oil inclusions can be analyzed by destructive bulk methods such as chromatography or mass spectrometry; the sample is crushed, heated, or leached to liberate the fluid (Murray, 1957; Bratus et al., 1975; Horsfield and McLimans, 1984). These methods have two main limitations: different generations of fluids are simultaneously recorded, and contamination of adsorbed fluids or solid organic matter can occur.

Infrared, Raman, and UV-fluorimetry microspectroscopic techniques have been used for in-situ analysis of individual oil inclusions (Barrès et al., 1987; Pironon and Barrès, 1990, 1992; Guilhaumou et al., 1990; Wopenka et al., 1990; Pironon and Pradier, 1992). Spectra are recorded on polished thin sections of rocks or separated natural and synthetic minerals. The major limitations of FTIR microspectroscopy are the size of the inclusion (which must be >15 μm) and the nature of the host crystal, as the spectra, recorded in the transmission mode, contain information issuing from both the inclusion and the crystal. The major limitation of conventional Raman microspectroscopy (in the visible-light range) is due to the intense level of fluorescence of the natural samples. This phenomenon can be attenuated using a FT-Raman microspectrometer with an excitation line in the near infrared range (Pironon et al., 1991). These spectroscopic techniques offer important information about the major molecular components of the oils trapped in the inclu-

0003–004X/94/0708–0712$02.00

sions. UV microspectrofluorimetry analyzes the aromatic fraction of the oils, which can be used as a biomarker and for approximating density values (McLimans, 1987; Bodnar, 1990). Microthermometry is used to analyze temperature phase modifications occurring inside the inclusions (Poty et al., 1976; Roedder, 1984).

Nuclear magnetic resonance (NMR) spectroscopy is the only nondestructive bulk technique of fluid inclusion analysis. The first documented application of this method was by Allègre (1961) who observed a weak signal corresponding to the protons of H_2O molecules present in inclusions of quartz veins from the Lodève rhyolitic complex (South Central Massif, France). More recently, various authors have studied inclusions by the NMR of different nuclei: ^{1}H (Kalinichenko et al., 1985; Klemm, 1986; Poty et al., 1987; Kohn et al., 1988), ^{23}Na, ^{27}Al, ^{29}Si, and ^{35}Cl (Sherriff et al., 1987; Kohn et al, 1988). It was observed that the ^{1}H NMR chemical shift in H_2O varies according to the H_2O molecule's environment and can be used as marker of pH and salinity (Poty et al., 1987).

Because of magnetic susceptibility broadening, fluids within porous media or inclusions might not give rise to high-resolution NMR spectra. The measurement of accurate chemical shifts normally used for chemical analysis is therefore difficult. This broadening effect can be reduced by rapidly spinning the sample at the magic angle (MAS). In order to avoid complications due to spinning sidebands, it is preferable to work at spinning speeds higher than the line width of the static sample, expressed in Hertz (Doskocilova et al., 1975; Stoll and Majors, 1981; Vanderhart et al., 1981; Garroway, 1982).

We report here the ^{1}H NMR analyses of oil and aqueous fluid inclusions in synthetic and natural crystals. The hydrocarbon functional groups can be characterized, and the fluid content can be quantified.

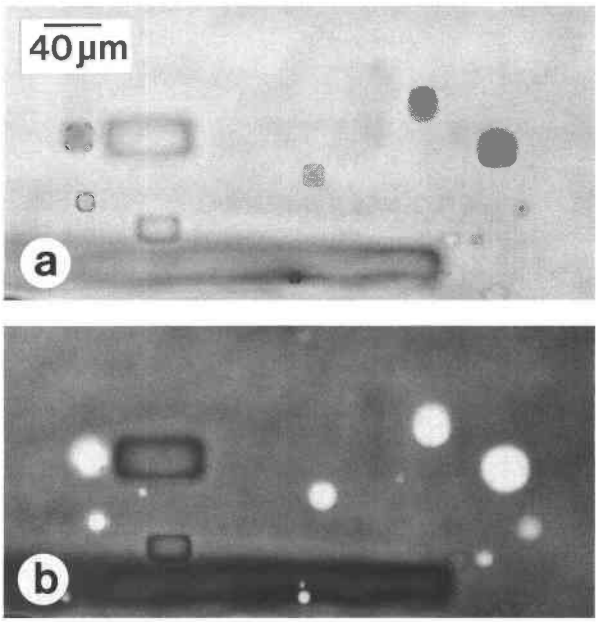

Fig. 1. Photomicrographs of fluid inclusions in a laboratory-grown crystal of sylvite synthesized with a natural oil from the western margin of Africa. Foreground: spherical oil inclusions; background: parallelepipedic aqueous inclusions. (**a**) Colored oil inclusions and colorless aqueous inclusions observed in transmitted visible light. (**b**) The same area as **a** with fluorescent oil inclusions and nonfluorescent aqueous inclusions observed under UV illumination.

Experimental methods

Samples

Following the procedure described by Pironon (1990), synthetic inclusions of toluene, isobutylbenzene, natural oil from west Africa and KCl-saturated water were trapped at atmospheric pressure in laboratory-grown crystals of sylvite. The temperature of entrapment was between 60 °C and room temperature. One cubic centimeter of crystals rich in hydrocarbon inclusions were collected. The size of the tabular crystals ranged from 1 to 2 mm. The shape of the hydrocarbon inclusions was spherical, whereas the aqueous inclusions had the form of a parallelepiped (Fig. 1) (Pironon, 1990). If a film of brine surrounded the spherical oil droplet, the inclusion looked like a cube. The volumetric ratio between hydrocarbon and water-bearing inclusions was estimated by optical measurements on 240 inclusions of six crystals. The water/hydrocarbon volumetric ratio was calculated by measuring the diameter of the spherical hydrocarbon inclusions and the two edges of the parallelepipedic aqueous inclusions. This ratio is approximately 96:4 vol%; the aqueous inclusions were more numerous and larger (average volume: 2×10^{-4} µL) than the hydrocarbon inclusions (average volume: 8×10^{-6} µL). The total fluid content occupied about 4% of the crystal volume.

Two natural samples from the sandstone reservoir of the Brent Formation of the North Sea basin were also analyzed. They were ground only slightly to prevent the fluid inclusions from fracturing and opening. The samples were cleaned in an ultrasonic tank to eliminate impurities at the surface of grains. A magnetic separator was used to eliminate any paramagnetic mineral fraction and so to collect pure quartz crystals. Adsorbed fluids were eliminated by heating them at 100 °C. Individual minerals, with sizes ranging from 0.5 to 2 mm, were collected. The use of crystal assemblages avoids the anisotropic effects induced by the shape of a monocrystal. In this case, hydrocarbon/water volumetric ratios could not be optically estimated because of the poor transparency of the quartz grains.

NMR studies

NMR spectra of the above specimens were obtained in our laboratory (CPMC-Belgium) on a Bruker CXP90 multinuclear solid-state FT spectrometer equipped with a MAS probe and an external field lock. The ^{1}H spectra were recorded at a frequency of 90.020 MHz, with the sample set at an angle of 54.7° to the magnetic field and

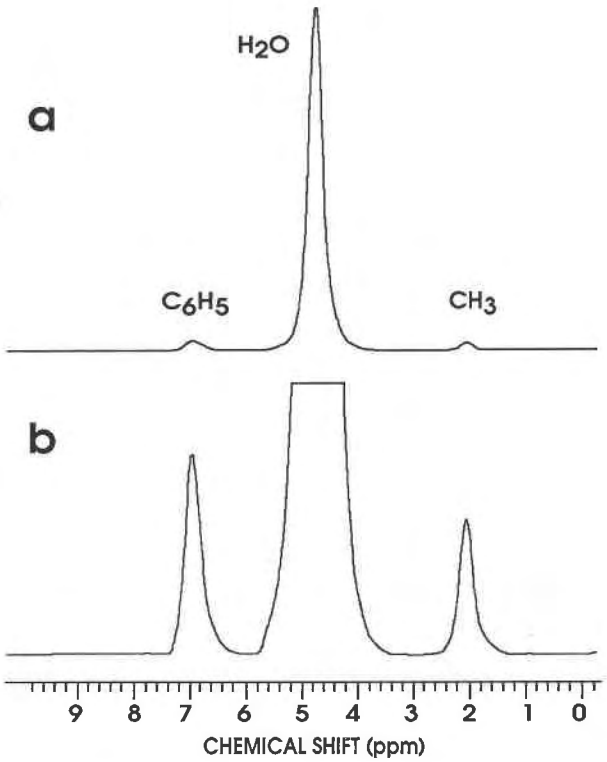

Fig. 2. The ^1H MAS NMR spectrum of toluene and KCl brine inclusions in synthetic sylvite (KCl) recorded with four K data points using a spectral width of 2500 Hz and 30° pulses; 2500 scans were accumulated with a relaxation delay of 20 s. The spectrum was Fourier transformed with 10-Hz line broadening. Spinning sidebands do not appear here, as they are located well outside the plotted region (at approximately ±16 ppm from the base peaks). (**a**) The spectrum; (**b**) 20× vertical expansion. The integrated intensities (not shown here) for the various peaks are proposed in Table 1.

spinning at a rate of 1500 Hz (which is much greater than the static line widths of 500 Hz). The spectra were analyzed under nonsaturating conditions with 30° flip-angle pulses and 20-s relaxation delays. The relaxation times of the various fluids were not measured, but the quantitative aspect of the measurement was checked by varying the relaxation delay. Depending on the fluid investigated, the relative peak intensities remained, within experimental error, constant for any delay >3–5 s. The experimental spectral width was set at 2000 Hz; all spectra were referenced to an external standard (TMS adsorbed on Al_2O_3) recorded under identical experimental conditions. The spectral frequencies are given in terms of chemical shift, which is a field-independent, dimensionless unit expressed in parts per million. All free induction decays were multiplied by an exponential function equivalent to a line broadening (LB); the values used are reported in the figure captions. Base-line curvature correction was used to improve the presentation of the spectra and to facilitate the integration of the various signal areas. This base-line correction was performed by manual adjustment of the coefficients of a fourth-order polynomial to match the shape of the base line. The value of the polynomial was then subtracted from each point of the spectrum. The natural oil used here was analyzed in our laboratory in the liquid form with a high-resolution Bruker AM-500 spectrometer with a line broadening of 1 Hz. To compare the spectrum with the one recorded on fluid inclusions, this line broadening was increased to 80 Hz.

FTIR studies

Fourier transform infrared (FTIR) microspectroscopy was applied to individual inclusions >15 μm using an A-590 Bruker microscope linked to an FTIR Bruker IFS 88 spectrometer. A globar source produced the infrared beam, and a MCT detector, cooled with liquid N_2, allowed the IR detection between 600 and 5000 cm^{-1} (Barrès et al., 1987). The spectra, presented in absorbance units and wavenumbers (cm^{-1}), were recorded in the transmission mode with a spectral resolution of 4 cm^{-1} after 400 accumulations. A chain-length coefficient was calculated by comparing the CH_3-CH_2 ratio of the sample to the same ratios measured on a standard *n*-alkane series (Pironon and Barrès, 1990).

Results

Well-defined spectra were obtained by the NMR MAS technique, and their characteristics are summarized in Table 1. A sample of sylvite containing toluene (C_6H_5-CH_3) and water (Fig. 2) shows a central peak attributed to H_2O ($\delta = 4.5$ ppm). The resonances at 1.8 and 6.7 ppm

Table 1. The ^1H NMR data for the synthetic and natural samples corresponding to the spectra presented in Figs. 2, 3, 4, and 6

	Toluene Fluid inclusions	Isobutylbenzene Fluid inclusions	Natural oil (west Africa)		Brent Formation (North Sea)	
			Free oil	Fluid inclusions	Fluid inclusions	Fluid inclusions
Figure	2	3	4a	4c	6a	6b
Spectrometer	CXP 90	CXP 90	AM500	CXP 90	CXP 90	CXP 90
LB (Hz)	10	10	1	80	80	80
Peaks (ppm)	1.8 4.5 6.7	0.9 1.8 2.4 4.5 7.1	1 1.4 2.5 7.5	1 1.4 2.5 4.5 7–7.5	0 0.4–2.5 4.8	0 0.4–2.5 4.8
Assignment	CH_3 H_2O C_6H_5	CH_3 CH CH_2 H_2O C_6H_5	CH_3 CH_2 CH H_{aro}	CH_3 CH_2 CH H_2O H_{aro}	CH_4 H_{ali} H_2O	CH_4 H_{ali} H_2O
Integral	3.2 163 5	5.3 1.5 2.0 694 5.0	38.9 77.7 4.9 4.8	41.5 73.5 5.9 1000 5.3	27 210 1000	10 163 1000
HC/H_2O vol%	7	3	—	10	15	10
$^1H_{ali}/^1H_{aro}$	0.6	1.7	25.3	23.0	—	—
CH_2/CH_3	0	0.6	3.0	2.7	—	—
$CH/\Sigma C_{ali}$	0	0.2	0.1	0.1	—	—
CH_4 (mol/L)	0	0	0	0	3.6	1.7

correspond, respectively, to the methyl and aromatic groups of toluene. The line width of the central peak, approximately 25 Hz, closely corresponds to the line width of 20–22 Hz found for a static sample of pure H_2O of identical size and in the same orientation relative to the magnetic field. The ratio of the integrals of the aliphatic (1.2–3 ppm) and aromatic (5.9–7.3 ppm) regions was calculated to be 0.6. The proportion of toluene and water contained in the inclusions may be obtained from the ratio of the integrals of the water and toluene peaks. The following equation gives the volumetric percentage of the organic phase in an oil-water binary mixture:

$$\frac{\frac{I_A \cdot m_A}{n_A \cdot D_A} \cdot 100}{\frac{I_A \cdot m_A}{n_A \cdot D_A} + \frac{I_B \cdot m_B}{n_B \cdot D_B}} = \text{vol\%}_A \qquad (1)$$

where A is the organic phase, B the water phase, I the integral of the NMR peak, m the atomic mass, n the number of protons, and D the density. Therefore, for a toluene density of 0.86 g/cm³ at 20 °C (Weast and Astle, 1979) and a toluene and water peak integral of 8.2 and 163, respectively, a toluene content of 7 vol% was calculated.

The spectrum of a synthetic sample with inclusions containing both KCl brine and isobutylbenzene [C_6H_5-CH_2-CH-$(CH_3)_2$] is shown in Figure 3. Four organic proton peaks are observed corresponding, respectively, to that of an aromatic ring at 7.1 ppm and to aliphatic chains between 0 and 2.8 ppm. The aliphatic spectral range can be decomposed into three clear regions: methyl protons at 0.9 ppm, methyne protons between 1.4 and 2.1 ppm, and methylene protons at 2.4 ppm. The integrals of the proton groups C_6H_5, CH_2, CH, and $(CH_3)_2$ are 5.0, 2.0, 1.5, and 5.3, respectively. Intensity ratios can be calculated as $^1H_{ali}/^1H_{aro} = 1.7$, $CH_2/CH_3 = 0.6$, and $CH/\Sigma C_{ali} = 0.2$. The CH_2-CH_3 ratio corresponds to the methylene to methyl group ratio and is calculated from the

$$\frac{\frac{I_{CH_2}}{2}}{\frac{I_{CH_3}}{3}}$$

integral ratio. $CH/\Sigma C_{ali}$ (close to the theoretical ratio of 0.25) corresponds to the contribution of branched C atoms of the aliphatic chain and is calculated from the following integral ratio:

$$\frac{I_{CH}}{\frac{I_{CH_3}}{3} + \frac{I_{CH_2}}{2} + I_{CH}}.$$

An intense water peak is also detected at 4.5 ppm. The contribution of the isobutylbenzene fraction (D = 0.85 g/cm³: Weast and Astle, 1979) was estimated from Equation 1 to be 3 vol% of the fluid content.

Spectra of inclusions synthesized with natural oil from the western margin of Africa were recorded and compared with those of the free oil. Two values of line broadening, 1 and 80 Hz, were used (Fig. 4). For the fluid inclusions, the water peak is found at 4.5 ppm, whereas the aliphatic oil fingerprint is located between 1 and 2.5 ppm. A weak aromatic contribution is also visible near 7 ppm. This oil is essentially aliphatic, with methyl protons at 1 ppm and methylene protons at 1.4 ppm. The small peak observed at 2.5 ppm could be assigned to methyl groups in an α position on an aromatic ring or to methyne protons of a saturated aliphatic chain. When one considers the low aromatic fraction of the oil, the second hypothesis is more likely.

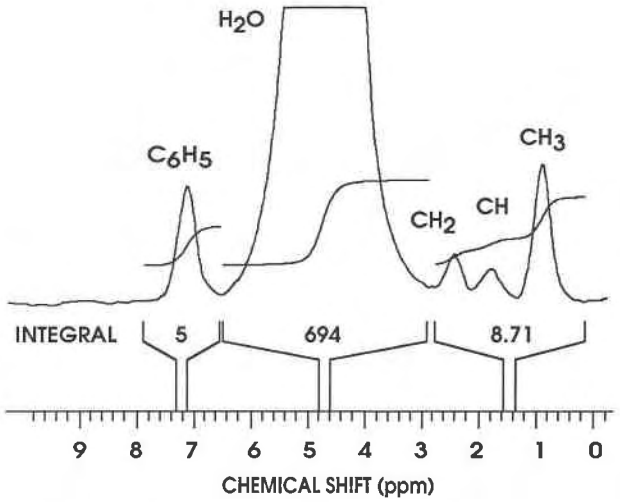

Fig. 3. The ^1H MAS NMR spectrum of isobutylbenzene and KCl brine inclusions in synthetic sylvite. Experimental conditions are as in Fig. 1. See Table 1 for integrated intensities in the aliphatic range.

We have tried to quantify the different integral ratios and have found for the free oil and inclusions the following values: $^1H_{ali}/^1H_{aro}$ = 25.3 and 23.0, CH_2/CH_3 = 3.0 and 2.7, respectively, and $CH/\Sigma C_{ali}$ = 0.1 for the two samples. These data are complementary to the FTIR parameters determined for the same samples (see Fig. 5). Infrared spectra confirm the low aromatic contribution and aliphatic character of the oil. The difference between the CH_2-CH_3 ratios measured from the IR spectra of the free oil and from those of the inclusions is due to the presence of KCl brine (Pironon and Barrès, 1992). From these data, an average chain-length coefficient (Pironon and Barrès, 1990) can be established and an oil composition approximated to n-dodecane (D = 0.75 g/cm³: Weast and Astle, 1979). Using Equation 1, the volume of oil trapped in the inclusions related to the water volume can therefore be estimated from the NMR data to be approximately 10 vol%.

The spectra of quartz crystals from two drill holes in the Brent Formation in the North Sea basin containing both water and oil inclusions are given in Figure 6. Spectrum a corresponds to inclusions from a gaseous reservoir, and spectrum b to inclusions from an oil reservoir. The water

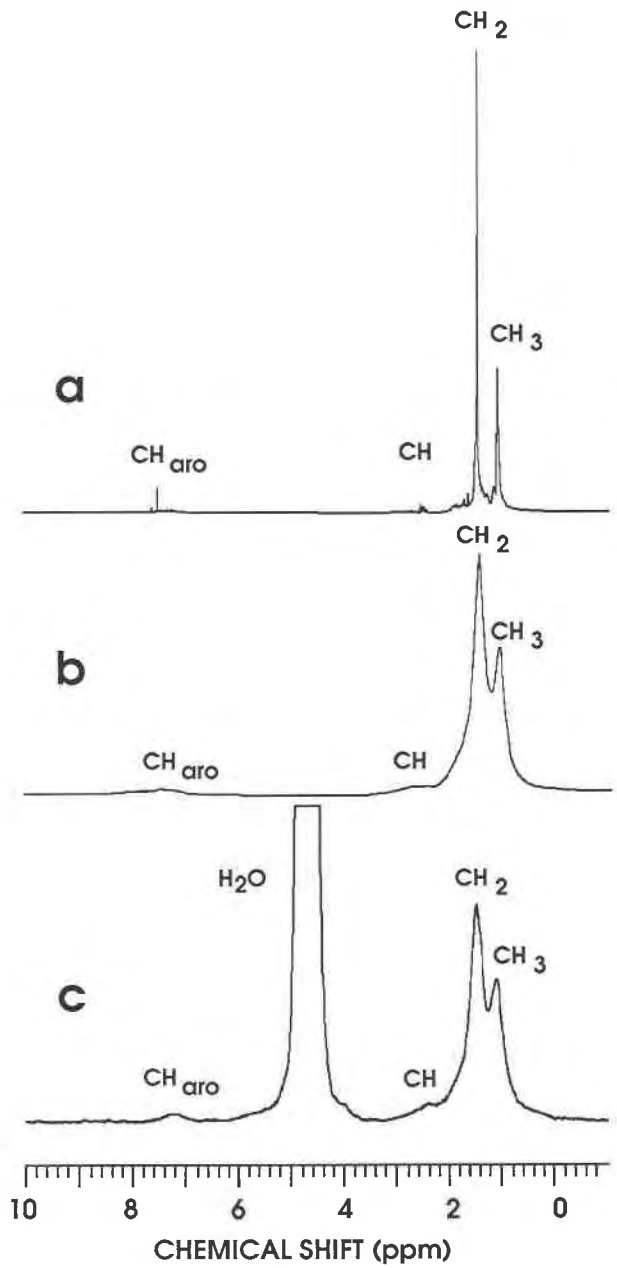

Fig. 4. The ^{1}H MAS NMR spectra of natural oil (west Africa), free and trapped in KCl brine inclusions in synthetic sylvite. (**a**) The pure liquid, high-resolution spectrum: 500 MHz, LB = 1 Hz; (**b**) the same but with LB = 80 Hz; (**c**) the spectrum of inclusions recorded at 90 MHz; the experimental conditions were as in Fig. 1 but with LB = 80 Hz. See Table 1 for integrated intensities.

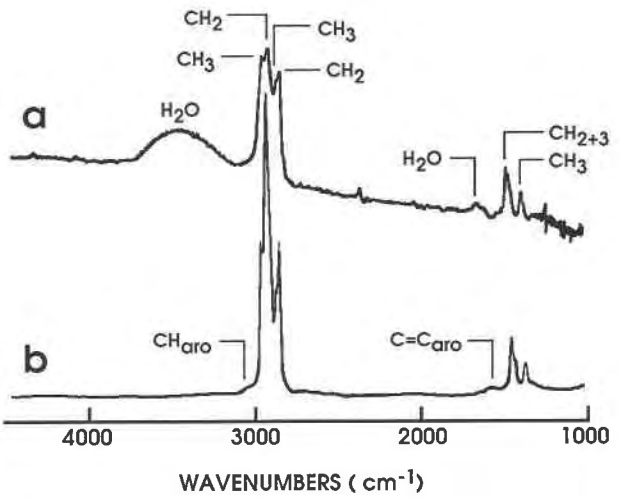

Fig. 5. (**a**) FTIR spectrum of natural oil (west Africa) and KCl brine inclusions in synthetic sylvite (KCl). (**b**) FTIR spectrum of free natural oil (west Africa) deposited on a CaF_2 slide, recorded with the infrared microscope and with the same configuration as spectrum **a**.

signal is between 3.5 and 5.5 ppm; those of the organic fraction are observed between 0 and 3.0 ppm. Compared with the water peak of the synthetic inclusion (KCl-saturated brine), the intense water peak is shifted toward higher chemical shifts. Possibly this is because the salinity of the brine (estimated from microthermometric measurements) is lower here (5 wt% of the NaCl equivalent). The water signal may be displaced according to (1) the concentration and nature of dissolved ions and (2) the difference in susceptibility among oil, crystal, and water (the anisotropic part is removed—not the isotropic part). The signal close to 0 ppm may be attributed to some methane gas dissolved in the organic fraction and concentrated in the gas phase of the inclusions. Signals between 0.5 and 2.5 ppm correspond to the proton resonances of, respectively, methyl, methylene, and methyne groups of the oil fraction. Because of the complexity of the organic phase and of limited resolution, no individual lines emerge clearly here. The oil contained in this sample is certainly aliphatic, as no absorption in the aromatic region was found. These results are in good agreement with the FTIR microanalysis results, which indicate an average aliphatic chain length of nine C atoms (*n*-nonane) and the presence of gases (methane and carbon dioxide). The relative amount of protons contained in the aqueous and oil-rich inclusions as obtained from the integrated intensities of the organic and water peaks allows us (using Eq. 1) to determine a volume of oil between 10 and 15 vol%; the oil composition can be approximated to *n*-nonane ($D = 0.72$ g/cm^3: Weast and Astle, 1979). From an average *n*-nonane composition of the oil, it is also possible to determine a molar concentration of methane (M_A) with Equation 2. Values close to 3.6 (spectrum a, Fig. 6) and 1.7 mol/L (spectrum b, Fig. 6) were obtained.

$$\frac{\frac{I_A}{n_A}}{\frac{I_B \cdot m_B}{n_B \cdot D'_B}} = M_A. \qquad (2)$$

Equation 2 corresponds to a modified Equation 1, where A is CH_4, B is C_9H_{20}, and D' is the density expressed in grams per liter.

Discussion

From an analysis of synthetic and natural fluid inclusions, the results obtained above confirm that ^1H NMR is capable of detecting and analyzing aqueous inclusions. The intensity of the H_2O peak is usually high, with a chemical shift value varying from 4.5 ppm for synthetic inclusions to 4.8 ppm for natural inclusions; these differences are probably due to varying salt concentration or composition or to pH. This study also shows that it is possible to detect liquid or gaseous oil phases trapped in minerals and to observe proton contributions (methane, methyl, methylene, methyne, aromatic) issuing from the organic molecules. The NMR MAS technique can therefore be used in a semiquantitative determination of the relative amount of fluids contained in inclusions (Table 1). An oil to water volumetric ratio can also be estimated. The relative amount found for water and hydrocarbon (between 3 and 10 vol%) is in agreement with optical estimations (approximately 4 vol% for the synthetic inclusions). In the case of natural oil mixtures, this ratio can be calculated using a pseudocomposition of the oil determined either by the NMR parameters of the oil or by the infrared chain-length coefficient.

Quantification of the organic phases trapped in inclusions should be compared with theoretical values (toluene and isobutylbenzene in our case) or with references obtained from free oil (here, natural oil from west Africa). It was found that the peak position of each proton group is close to the theoretical or reference chemical shift. Several peak integral ratios have been compared: the $^1H_{ali}$-$^1H_{aro}$ ratios for toluene (0.6), isobutylbenzene (1.7), and natural oil (25.3) in inclusions are close to the theoretical and reference values of 0.6, 1.8, and 23.0, respectively.

The experimental intensity ratios (5.0; 2.0; 1.5; 5.3) found for isobutylbenzene [C_6H_5; CH_2; CH; $(CH_3)_2$] do not compare as favorably as above with the theoretical values (5; 2; 1; 6); this is probably because of overlapping of peaks resulting from limited resolution. Errors are therefore more important for the smaller peak, i.e., the methyne group.

The CH_2-CH_3 ratio for the isobutylbenzene inclusions (0.6) is not too far from the theoretical value (0.5). This error is similar for the natural west Africa oil, as seen from the spectrum recorded on free oil at LB = 1 Hz (3.0) and the spectrum recorded on the fluid inclusion at LB = 80 Hz (2.7). The spectrum of the free oil recorded at LB = 80 Hz is, in fact, similar to the spectrum recorded for the inclusion; this tends to show that the difference between the theoretical CH_2-CH_3 ratios and those measured for the inclusions comes essentially from an overlapping of peaks. This difference could be reduced in principle by either using a decomposition procedure of the considered spectral range or increasing the sensitivity. This CH_2-CH_3 ratio cannot, however, be compared with the chain-length coefficient measured by FTIR spectroscopy. By NMR, all the methyl contributions are taken into account, whereas the IR coefficient only considers the methyl groups that are on an end-position in the chain.

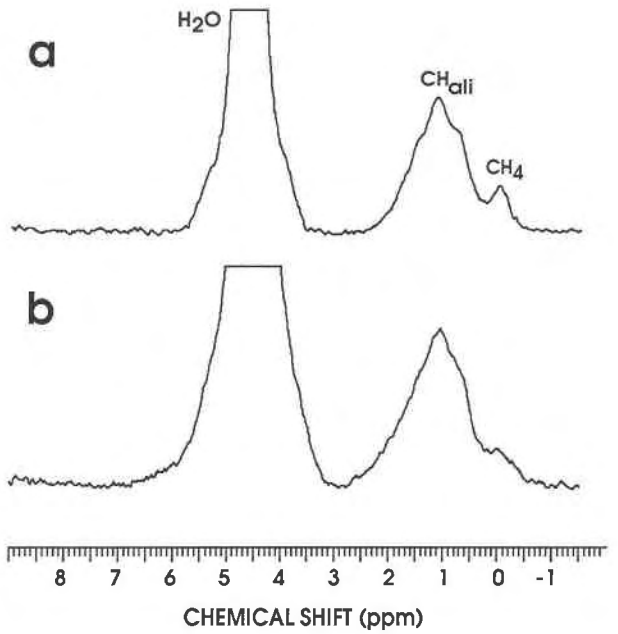

Fig. 6. The ^1H MAS NMR spectra of natural aqueous and hydrocarbon inclusions in quartz grains from two drill holes of the Brent sandstone reservoir of the North Sea basin. (**a**) A sample from a gas reservoir; (**b**) a sample from an oil reservoir. The experimental conditions were as in Fig. 1 except LB = 4 Hz. See Table 1 for integrated intensities.

Even if the volumetric concentration of oil in the natural quartz samples of the North Sea basin is higher (10–15 vol%), the spectral resolution found for these samples is poorer than for the synthetic sylvite crystals. This could be caused by paramagnetic impurities (inside or on the edges of the crystals) that were not totally eliminated during sample preparation. Such poor resolution prevents accurate quantitative estimations of the aliphatic fraction and aromatic to aliphatic ratio of the oil.

Conclusions

The use of synthetic inclusions shows the analytical ability of ^1H MAS NMR in the study of fluid inclusions trapped in minerals. The detection and differentiation of the organic functions of oil simultaneously trapped with a water phase are possible by in-situ analyses. Water and oil ^1H NMR peaks were clearly separated. The contribution of solid organic matter in fractures or at the surface of crystals was not taken into account by this analytical procedure. The technique was nondestructive and led to a quantification of volumetric ratios, such as water/oil, aliphatic/aromatic, and CH_2/CH_3, of the branch rate of the aliphatic chain, and of the methane content. With good spectral resolution (i.e., no peak overlapping), the aliphatic functions can be estimated. An increase in resolution and sensitivity should provide a better understanding of the complex oil mixture in natural inclusions, i.e., its average aliphatic composition with a defined branch rate and its aromatic and methane content. These

parameters can be used, therefore, in establishing a pseudocomposition of the oil mixture, which is of use for a thermobarometric modeling of the history of petroleum basins and for understanding oil evolution. Nevertheless, the analysis of inclusions by ^{1}H NMR has some limitations: (1) The sample must be free of paramagnetic crystals and impurities that decrease the spectral resolution by a broadening of peaks. (2) One cubic centimeter of crystals (with a grain size from 0.5 to 2 mm) must be collected; bigger crystals increase the anisotropic effect and therefore decrease the spectral resolution. (3) No internal reference can be used: the location of the peak is approximate, resulting in indeterminate chemical shift values. (4) Different generations of inclusions within the same crystal cannot be directly separated in the NMR spectrum. The study of inclusions by ^{1}H NMR spectroscopy can be improved by using higher magnetic fields or more efficient probes.

Acknowledgments

This work was supported by an EEC grant (TH.01.133/89), Elf Aquitaine, and Total. The authors wish to thank O. Barrès, from the LEM laboratory (URA-CNRS 235, Nancy, France) for her help during infrared measurements, and B.L. Sherriff, T. Mernagh, and P. Brown, for their constructive reviewing.

References cited

Allègre, C. (1961) De l'application de la résonance paramagnétique nucléaire à l'étude des inclusions fluides. Compte rendu sommaire des séances de la Société Géologique de France, June, 178–179.

Barrès, O., Burneau, A., Dubessy, J., and Pagel, M. (1987) Application of micro-FT-IR spectroscopy to individual hydrocarbon fluid inclusion analysis. Applied Spectroscopy, 41, 1000–1008.

Bodnar, R.J. (1990) Petroleum migration in the Miocene Monterey Formation, California, USA: Constraints from fluid inclusion studies. Mineralogical Magazine, 54, 295–304.

Bratus, M.D., Svoren, I.M., and Danysh, V.V. (1975) Inclusions of hydrocarbons in "Marmorosh diamonds" from Carpathians as indicators of migration of oil fluids: Carbon and its compounds in endogenic processes of mineral formation (abs.). COFFI, 8, 28.

Doskocilova, D., Dang Due Tao, and Schneider, B. (1975) Effects of macroscopic spinning upon linewidth of NMR signals of liquids in magnetically inhomogeneous systems. Czechoslovak Journal of Physics, B25, 202–209.

Garroway, A.N. (1982) Magic angle sample spinning of liquids. Journal of Magnetic Resonance, 49, 168–171.

Guilhaumou, N., Szydlowskii, N., and Pradier, B. (1990) Characterization of hydrocarbon fluid inclusions by infrared and fluorescence microspectrometry. Mineralogical Magazine, 54, 311–324.

Horsfield, B., and McLimans, R.K. (1984) Geothermometry and geochemistry of aqueous and oil-bearing fluid inclusions from Fateh Field, Dubai. Organic Geochemistry, 6, 733–740.

Kalinichenko, A.M., Pasal'skaya, L.F., Matyash, I.V., and Ya Proshko, V. (1985) Investigation of the composition of the fluid phase of inclusions by the methods of PMR and gas chromatography (abs.). Fluid Inclusion Research, 19, 199–200.

Klemm, W. (1986) A survey of chemical analysis of gas-fluid inclusions (abs.). Fluid Inclusion Research, 19, 219–220.

Kohn, S.C., Dupree, R., and Franan, I. (1988) Volatiles in silicate glasses: A magic angle spinning NMR study (abs.). Terra Cognita, 8, 68–69.

McLimans, R. (1987) The application of fluid inclusions to migration of oil and diagenesis in petroleum reservoirs. Applied Geochemistry, 2, 585–603.

Murray, R.C. (1957) Hydrocarbon fluid inclusions in quartz. AAPG Bulletin, 41, 950–956.

Pironon, J. (1990) Synthesis of hydrocarbon fluid inclusions at low temperature. American Mineralogist, 75, 226–229.

Pironon, J., and Barrès, O. (1990) Semi-quantitative FT-IR microanalysis limits: Evidence from synthetic hydrocarbon fluid inclusions in sylvite. Geochimica et Cosmochimica Acta, 54, 509–518.

——— (1992) Influence of brine-hydrocarbon interactions on FT-IR microspectroscopic analyses of intracrystalline liquid inclusions. Geochimica et Cosmochimica Acta, 56, 169–174.

Pironon, J., and Pradier, B. (1992) UV-fluorescence alteration of hydrocarbon fluid inclusions. Organic Geochemistry, 18, 501–509.

Pironon, J., Sawatzki, J., and Dubessy, J. (1991) NIR FT-Raman microspectroscopy of fluid inclusions: Comparisons with VIS Raman and FT-IR microspectroscopies. Geochimica et Cosmochimica Acta, 55, 3885–3891.

Poty, B., Leroy, J., and Jackimowicz, L. (1976) Un nouvel appareil pour la mesure des températures sous le microscope: L'Installation de microthermométrie Chaixmeca. Bulletin de la Société française de Minéralogie et Cristallographie, 99, 182–186.

Poty, B., Dereppe, J.M., Landais, P., and Pironon, J. (1987) Use of ^{1}H NMR for discrimination of solutions having different proton concentration. Application to fluid inclusions. ECROFI Porto, Abstract with Program, 38.

Roedder, E. (1984) Fluid inclusions. Mineralogical Society of America Reviews in mineralogy, 12, 644 p.

Sherriff, B.L., Grundy, H.D., and Hartman, J.S. (1987) Analysis of fluid inclusions using nuclear magnetic resonance. Geochimica et Cosmochimica Acta, 51, 2233–2235.

Stoll, M.E., and Majors, T.J. (1981) Elimination of magnetic susceptibility broadening in NMR using magic angle sample spinning to measure chemical shift in NbHxI. Physical Review B, 24(2), 2859–2862.

Vanderhart, D.L., Earl, W.L., and Garroway, A.N. (1981) Resolution in ^{13}C NMR of organic solids using higher power proton decoupling and magic angle spinning. Journal of Magnetic Resonance, 44, 361–401.

Weast, R.C., and Artle, M.J. (1979) Handbook of chemistry and physics (60th edition), 2450 p. CRC Press, Boca Raton, Florida.

Wopenka, B., Pasteris, J.D., and Freeman, J.J. (1990) Analysis of individual fluid inclusions by Fourier transform infrared and Raman microspectroscopy. Geochimica et Cosmochimica Acta, 54, 519–533.

Manuscript received April 6, 1993
Manuscript accepted March 7, 1994